Internucleotide Scalar Couplings Across Hydrogen Bonds in Watson−Crick and Hoogsteen Base Pairs of a DNA Triplex

Andrew J. Dingley,[||] James E. Masse,[⊥] Robert D. Peterson,[⊥] Michael Barfield,*[,§,#] Juli Feigon,*[,‡,⊥] and Stephan Grzesiek*[,†,||]

Contribution from the Institute of Physical Biology, Heinrich-Heine-Universität, 40225 Düsseldorf, Germany, Institute of Structural Biology, IBI-2, Forschungszentrum Jülich, 52425 Jülich, Germany, Department of Chemistry and Biochemistry and Molecular Biology Institute, University of California, Los Angeles, California 90095-1569, and Department of Chemistry, University of Arizona, Tucson, Arizona 85721

Received March 15, 1999. Revised Manuscript Received April 30, 1999

Abstract: An extensive analysis of trans-hydrogen bond $^{2h}J_{NN}$ and $^{1h}J_{HN}$ scalar couplings, the covalent $^{1}J_{HN}$ couplings, and the imino proton chemical shifts is presented for Hoogsteen−Watson−Crick T•A−T and C^{+}•G−C triplets of an intramolecular DNA triplex. The $^{2h}J_{NN}$ coupling constants for the Watson−Crick base pairs have values ranging from 6 to 8 Hz, while the Hoogsteen base paired thymines and protonated cytidines have values of approximately 7 and 10 Hz, respectively. Distinct decreases of $^{2h}J_{NN}$ are observed at the triplex strand ends. Trans-hydrogen bond *J* correlations ($^{1h}J_{HN}$) between the donor ^{1}H nucleus and the acceptor ^{15}N nucleus are observed for this triplex by a novel, simple quantitative *J*-correlation experiment. These one-bond $^{1h}J_{HN}$ couplings range between 1 and 3 Hz. A strong correlation is found between the chemical shift of the imino proton and the size of $^{2h}J_{NN}$, with stronger *J* couplings corresponding to downfield chemical shifts. A similar, but inverse correlation is found between the proton chemical shift and the (absolute) size of the covalent $^{1}J_{HN}$ constant. Methods of density functional theory were used to investigate the structural requirements for scalar *J* coupling and magnetic shielding associated with hydrogen bonding in nucleic acid base pairs. The dependencies of these NMR parameters on hydrogen bond distances were obtained for a representative base pair fragment. The results reproduce the trans-hydrogen bond coupling effect and the experimental correlations and suggest that the NMR parameters can be used to gain important insight into the nature of the hydrogen bond.

Introduction

Hydrogen bonds are essential for the stabilization of protein and nucleic acid secondary structure and often play a fundamental role in the regulation of enzymatic reactions.[1−3] There are a number of NMR parameters which provide insight into the nature of the electron cloud of the hydrogen bond and its interaction with the nuclei of the donor and acceptor groups (see review article by Becker[4]). In a previous study, we demonstrated that hydrogen bonds in Watson−Crick base pairs of a ^{15}N-labeled 69-nucleotide RNA domain can be observed directly by a two-bond trans-hydrogen bond scalar coupling ($^{2h}J_{NN}$) of approximately 7 Hz between the imino ^{15}N atom of the donor base and the hydrogen bond acceptor ^{15}N atom on the complementary base.[5] In addition to providing direct evidence for hydrogen bonding, the $^{2h}J_{NN}$ coupling experiment also provides valuable interstrand assignment information. This $^{2h}J_{NN}$ observation has been extended to a 14 base pair ^{15}N-labeled DNA duplex that exhibits very similar *J*-coupling values.[6] In the DNA duplex, one-bond trans-hydrogen bond couplings ($^{1h}J_{HN}$) in the range of 2−4 Hz could also be observed between the proton and the acceptor nitrogen which were undetectable in the larger 69-mer RNA domain due to the fast relaxation of the imino protons. The quantification of the $^{2h}J_{NN}$ coupling in RNA showed that, on average, uridine−adenosine (U−A) base pairs have slightly larger $^{2h}J_{NN}$ values when compared with guanosine−cytidine (G−C) base pairs. This stronger coupling in U−A base pairs coincides with a shorter N−N distance observed in crystal structures.

Analogous two-bond and one-bond couplings across hydrogen bonds have recently been observed in a complex of HF and 2,4,6-trimethylpyridine[7] as well as in hydrogen-bonded clusters of F^{-} and $(HF)_n$.[8] In the latter study, stronger $^{2h}J_{FF}$ couplings also coincide with shorter distances between the fluorines and quantum mechanical calculations were shown to reproduce the

[||] Heinrich-Heine-Universität and Forschungszentrum Jülich.
[⊥] University of California.
[#] University of Arizona.
[§] Address correspondence to this author at the University of Arizona. Phone: +1 520 621 6348. FAX: +1 520 621 8407. E-mail: barfield@u.arizona.edu.
[‡] Address correspondence to this author at the University of California. Phone: +1 310 206 6922. FAX: +1 310 825 0982. E-mail: feigon@mbi.ucla.edu
[†] Address correspondence to this author at the Institute of Structural Biology. Phone: +49 2461 61 5874. FAX: +49 2461 61 2020. E-mail: s.grzesiek@fz-juelich.de.

(1) Saenger, W. *Principles of Nucleic Acid Structure*; Cantor, C. R., Ed.; Springer: New York, 1984.
(2) Fersht, A. *Enzyme Structure and Mechanism*, 2nd ed.; W. H. Freeman: New York, 1985.
(3) Jeffrey, G. A.; Saenger, W. *Hydrogen Bonding in Biological Structures*; Springer: New York, 1991.
(4) Becker, E. D. *Encyclopedia of Nuclear Magnetic Resonance*; Grant, D. M., Harris, R. K., Eds.; John Wiley: New York, 1996; pp 2409−2415.
(5) Dingley, A. J.; Grzesiek, S. *J. Am. Chem. Soc.* **1998**, *120*, 8293−8297.
(6) Pervushin, K.; Ono, A.; Fernandez, C.; Szyperski, T.; Kainosho, M.; Wüthrich, K. *Proc. Natl. Acad. Sci U.S.A.* **1998**, *95*, 14147−14151.
(7) Golubev, N. S.; Shenderovich, I. G.; Smirnov, S. N.; Denisov, G. S.; Limbach, H.-H. *Chem. Eur. J.* **1999**, *5*, 492−497.
(8) Shenderovich, I. G.; Smirnov, S. N.; Denisov, G. S.; Gindin, V. A.; Golubev, N. S.; Dunger, A.; Reibke, R.; Kirpekar, S.; Malkina, O. L.; Limbach, H.-H. *Ber. Bunsen-Ges. Phys. Chem.* **1998**, *102*, 422−428.

10.1021/ja9908321 CCC: $18.00
Published on Web 06/15/1999

experimental observations to a large extent. More recently, trans-hydrogen bond scalar couplings ($^{3h}J_{NiC'j}$) have also been observed in proteins.[9] These three-bond couplings are active between an amide ^{15}N nucleus of residue *i* and the ^{13}C′ nucleus of residue *j*, where the carbonyl oxygen atom acts as an acceptor for the amide proton of residue *i*. Similar to the correlation of trans-hydrogen bond *J* couplings and distance in nucleic acids and the fluorine complexes, stronger $^{3h}J_{NiC'j}$ couplings correspond to shorter hydrogen bond distances in proteins.[9]

In the present study, we report quantitative $^{2h}J_{NN}$ correlations between the donor and acceptor nitrogen nuclei of Watson−Crick and Hoogsteen[10,11] base pairs in an intramolecular DNA triplex.[12] The nucleotide sequence of this 32-mer DNA consists of one purine and two pyrimidine "strands" connected by linker nucleotides which form canonical Hoogsteen−Watson−Crick T•A−T and C$^+$•G−C triplets (Figure 1). In the three-dimensional structure, the first two strands are antiparallel and Watson−Crick base paired whereas the third pyrimidine strand is in an orientation parallel to that of the central purine strand and Hoogsteen base paired in the major groove of the Watson−Crick duplex. The sequence of the nucleotides in the base triplets is identical with the sequence of a related triplex with non-nucleotide loops, for which a structure was recently determined.[13] In addition to the two-bond $^{2h}J_{NN}$ coupling constants in this DNA triplex, we report values for the one-bond trans-hydrogen bond *J* correlations ($^{1h}J_{HN}$) between the proton and the nitrogen acceptor nucleus. These coupling constants were obtained by a novel method with a simple modification of a conventional water flip-back [^{1}H-^{15}N]-HSQC experiment.

For proteins, it is well established that the isotropic[14−18]and the anisotropic chemical shift[19,20] of amide protons are strongly influenced by the strength of the hydrogen bond. In particular, shorter hydrogen bond lengths ($R_{H\cdots O}$) correspond to larger values for the isotropic[15] and anisotropic chemical shift.[20] In this study, we show that for all four base pair types of the DNA triplex, a downfield shift of the imino proton in nucleic acid bases correlates with an increase in the trans-hydrogen bond $^{2h}J_{NN}$ coupling constant. In addition, a strong correlation is observed between the imino proton chemical shift and the value of the (covalent) imino group scalar coupling ($^1J_{NH}$). A downfield shift of the proton corresponds to smaller (absolute size) $^1J_{NH}$ values.

It was of interest to investigate the electronic and structural features associated with the trans-hydrogen bond scalar coupling constants and the experimentally found correlations to the chemical shift. For this reason, scalar couplings and chemical shieldings were calculated for a 16-atom fragment containing the N1(G)−N3(C) hydrogen bonding region of a G−C base pair by using density functional theory[21,22] (DFT), finite perturbation theory[23,24] (FPT), and GIAO[25] (gauge including atomic orbital) methods. These calculations closely reproduce the experimental trans-hydrogen bond $^{2h}J_{NN}$ and $^{1h}J_{HN}$ values and explain these unusual scalar couplings theoretically. In addition, dependencies of chemical shifts and coupling constants on the R_{N1-H1} and $R_{N1\cdots N3}$ distances were obtained for this representative base pair fragment from the DFT calculations. The results are completely consistent with the experimental

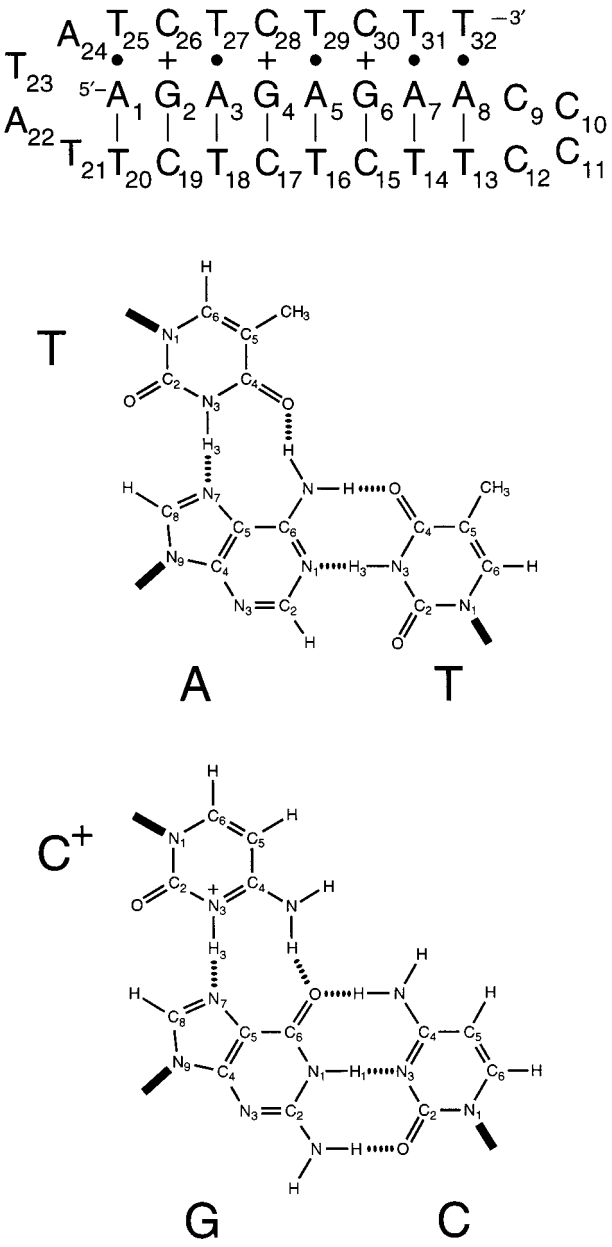

Figure 1. Top: Sequence and base pairing scheme of the intramolecular DNA triplex. Hydrogen-bonded base pairs are indicated by the symbols —, •, and + for Watson−Crick, Hoogsteen T•A, and Hoogsteen C$^+$•G base pairs, respectively. Bottom: Chemical structures of T•A−T and C$^+$•G−C triplets.

(9) (a) Cordier, F.; Grzesiek, S. *J. Am. Chem. Soc.* **1999**, *121*, 1601−1602. (b) Cornilescu, G.; Hu, J.-S.; Bax, A. *J. Am. Chem. Soc.*, **1999**, *121*, 2949−2950.
(10) Hoogsteen, K. *Acta Crystallogr.* **1959**, *12*, 822−823.
(11) Hoogsteen, K. *Acta Crystallogr.* **1963**, *16*, 907−916.
(12) Sklenar, V.; Feigon, J. *Nature* **1990**, *345*, 836−838.
(13) Tarköy, M.; Phipps, A. K.; Schultze, P.; Feigon, J. *Biochemistry* **1998**, *37*, 5810−5819.
(14) Pardi, A.; Wagner, G.; Wüthrich, K. *Eur. J. Biochem.* **1983**, *137*, 445−54.
(15) Wagner, G.; Pardi, A.; Wüthrich, K. *J. Am. Chem. Soc.* **1983**, *105*, 5948−5949.
(16) Wishart, D. S.; Sykes, B. D.; Richards, F. M. *J. Mol. Biol.* **1991**, *222*, 541−546.
(17) Kuntz, I. D.; Kosen, P. A.; Craig, E. C. *J. Am. Chem. Soc.* **1991**, *113*, 1406−1408.
(18) Zhou, N. E.; Zhu, B.-Y.; Sykes, B. D.; Hodges, R. S. *J. Am. Chem. Soc.* **1992**, *114*, 4320−4326.
(19) Tessari, M.; Vis, H.; Boelens, R.; Kaptein, R.; Vuister, G. W. *J. Am. Chem. Soc.* **1997**, *119*, 8985−8990.
(20) Tjandra, N.; Bax, A. *J. Am. Chem. Soc.* **1997**, *119*, 8076−8082.
(21) Hohenberg, P.; Kohn, W. *Phys. Rev. B* **1964**, *136*, 864−871.
(22) Kohn, W.; Sham, L. J. *Phys. Rev. A* **1965**, *140*, 1133−1138.
(23) Pople, J. A.; McIver, J. J. W.; Ostlund, N. S. *J. Chem. Phys.* **1968**, *49*, 2960−2964.
(24) Pople, J. A.; McIver, J. J. W.; Ostlund, N. S. *J. Chem. Phys.* **1968**, *49*, 2965−2970.
(25) For general reviews of theory of magnetic shielding see, for example: Jameson, C. J. In *Nuclear Magnetic Resonance*; Specialist Periodical Reports; The Chemical Society: London, 1997; No. 26 and previous chapters in this series.

trends and establish that both R_{N1-H1} and $R_{N1\cdots N3}$ strongly influence the values of $^{2h}J_{NN}$ and $^{1}J_{HN}$ and the chemical shift of the imino proton. This suggests that the couplings and proton shifts are important parameters for the structural characterization of the hydrogen bond.

Materials and Methods

NMR experiments were performed on a uniformly ^{13}C,^{15}N-labeled, single-stranded 32 nucleotide DNA d(AGAGAGAACC CCTTCTCTCT TATATCTCTC TT), where the underlined nucleotides form the two loops in the intramolecular triplex (Figure 1). The enzymatic synthesis of the DNA for this sample has been described previously.[26] A 250 μL sample volume was used in a Shigemi microcell containing 1.5 mM DNA oligonucleotide, 100 mM NaCl, 5 mM $MgCl_2$, and 95% H_2O/5% D_2O at pH 5.3. All NMR data were acquired at 5 °C on Bruker DRX-600 or DRX-500 NMR spectrometers. Both spectrometers were equipped with standard 5 mm triple-axis pulsed field gradient $^{1}H/^{15}N/^{13}C$ probeheads optimized for ^{1}H detection.

The quantitative J_{NN} HNN-COSY experiment[5] was used to measure the homonuclear $^{15}N-^{15}N$ trans-hydrogen bond coupling constants for the DNA triplex. The data matrix consisted of 250*(t_1) × 1024*(t_2) data points (where n* refers to complex points) with acquisition times of 45 (t_1) and 85 ms (t_2). A total of 224 scans per complex t_1 increment was collected. The total measuring time was 20.1 h. The experiment was performed at a ^{1}H resonance frequency of 500.13 MHz, with the ^{1}H carrier positioned on the H_2O resonance, the ^{15}N carrier at 185 ppm, and the ^{13}C carrier at 145 ppm. Radio frequency power levels for high-power ^{1}H and ^{15}N pulses were 24 and 10 kHz, respectively. Garp decoupling (3.3 kHz) was applied during the ^{15}N t_1 period on the ^{13}C channel. As previously described, the size of the $^{2h}J_{NN}$ couplings was determined from the intensity ratio of observed cross and diagonal peaks.[5]

The quantitative J_{HN} [^{1}H-^{15}N]-HSQC experiment depicted in Figure 4 was recorded with the inclusion of WATERGATE[27] and water flip-back[28] pulses to protect the magnetization of the imino protons against loss due to the fast exchange with the water. Data matrices consisted of 100*(t_1) × 512*(t_2) data points with acquisition times of 16 (t_1) and 36 ms (t_2). The experiments were performed at a ^{1}H resonance frequency of 600.13 MHz. A total of 1024 scans per complex t_1 increment was collected for pulse scheme A, whereas 16 scans were accumulated in the reference experiment B (Figure 4). The total measuring time for such a pair of experiments was 36.3 h.

The recently described doublet-separated sensitivity enhanced (DSSE) [^{1}H-^{15}N]-HSQC experiment[29,30] was used to measure the scalar one-bond imino and iminium ion group couplings ($^{1}J_{NH}$). The 2D DSSE ^{1}H-^{15}N spectra were collected with 100*(t_1) × 1024*(t_2) data points with acquisition times of 50 (t_1) and 77 ms (t_2). A total of 64 scans per complex t_1 increment was collected. The experimental time was 2.3 h. The experiment was performed at a ^{1}H resonance frequency of 600.13 MHz, with the ^{1}H carrier positioned on the H_2O resonance, the ^{15}N carrier at 152 ppm, and the ^{13}C carrier at 145 ppm. All regular ^{1}H and ^{15}N pulses were applied at an radio frequency field strength of 29 and 6.3 kHz, respectively. Garp decoupling (3.3 kHz) was applied during the ^{15}N t_1 period on the ^{13}C channel.

NMR data sets were processed with the program nmrPipe[31] and peak positions and integrals were determined with the programs PIPP[32] and the time domain fitting routine nlinLS contained in the NMRPipe package.

Density functional theory methods were used to calculate scalar couplings and chemical shifts for G−C and U−A base pairs. Coordinates for the heavy atoms were taken from the 1.16 Å X-ray structure of an acceptor stem of tRNAAla from *E. coli* (NDB entry AR0009).[33] The hydrogen atoms were included and their positions were fully optimized at the B3PW91/6-31G** level. To explore the dependence of NMR parameters on structural factors, a 16-atom fragment was clipped out of the second Watson−Crick G−C base pair of NDB entry AR0009. This was considered to be representative of the hydrogen bonding region. The only modification in the hydrogen bonding region was to assume a linear N1−H1···N3 hydrogen bond. The position of the hydrogen-bonded H1 proton (R_{N1-H1}) and the distances between the sections of the fragment (in terms of the hydrogen bond distance $R_{N1\cdots N3}$) were systematically varied. The Fermi contact contributions to the scalar coupling constants were based on FPT,[23,24] and were obtained indirectly from Gaussian 94[34] via the FIELD option.[23] All coupling constants were computed by using the unrestricted DFT UB3PW91/6-311G** triple-split level with polarization functions on hydrogens and heavier elements.[35] The B3PW91 method of DFT makes use of Becke's three-parameter exchange functional[36] and the gradient

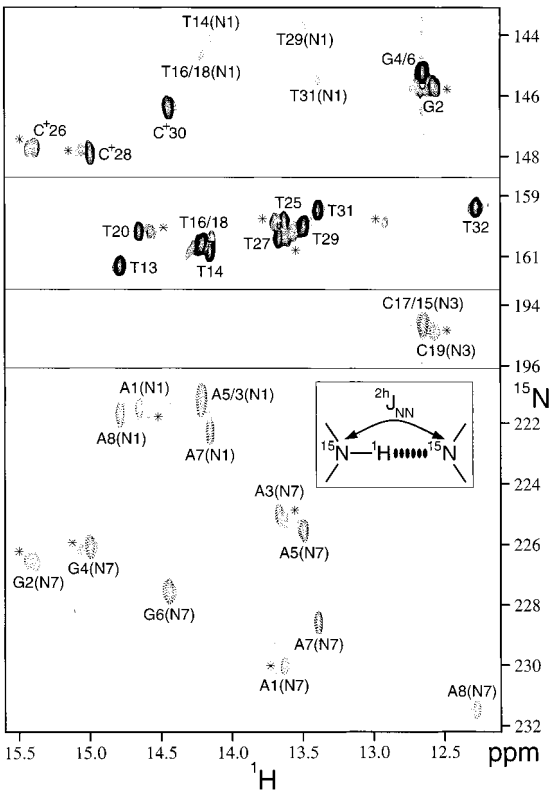

Figure 2. Quantitative J_{NN} HNN-COSY spectrum of the uniformly $^{13}C/^{15}N$-labeled intramolecular DNA triplex. Positive contours depict diagonal resonances, and negative contours (dashed lines) correspond to cross-peaks resulting from scalar $^{15}N-^{15}N$ magnetization transfer. Resonances are labeled with assignment information. The insert in the bottom panel illustrates the definition of the trans-hydrogen-bond $^{2h}J_{NN}$ correlation. Resonances marked with an asterisk are a result of a second minor conformation of the DNA triplex.

(26) Masse, J. E.; Bortmann, P.; Dieckmann, T.; Feigon, J. *Nucleic Acids Res.* **1998**, *26*, 2618−2624.
(27) Piotto, M.; Saudek, V.; Sklenar, V. *J. Biomol. NMR* **1992**, *2*, 661−665.
(28) Grzesiek, S.; Bax, A. *J. Am. Chem. Soc.* **1993**, *115*, 12593−12594.
(29) Andersson, P.; Annila, A.; Otting, G. *J. Magn. Reson.* **1998**, *133*, 364−367.
(30) Cordier, F.; Dingley, A. J.; Grzesiek, S. *J. Biomol. NMR* **1999**, *13*, 175−180.
(31) Delaglio, F.; Grzesiek, S.; Vuister, G. W.; Zhu, G.; Pfeifer, J.; Bax, A. *J. Biomol. NMR* **1995**, *6*, 277−293.
(32) Garrett, D. S.; Powers, R.; Gronenborn, A. M.; Clore, G. M. *J. Magn. Reson.* **1991**, *95*, 214−220.
(33) Müller, U.; Schübel, H.; Sprinzl, M.; Heinemann, U. To be submitted for publication.
(34) Frisch, M. J.; Trucks, G. W.; Schlegel, H. B.; Gill, P. M. W.; Johnson, B. G.; Robb, M. A.; Cheeseman, J. R.; Keith, T. G.; Petersson, A.; Montgomery, J. A.; Raghavachari, K.; Al-Laham, M. A.; Zakrzewski, V. G.; Ortiz, J. V.; Foresman, J. B.; Cioslowski, J.; Stefanov, B. B.; Nanayakkaara, A.; Challacombe, M.; Peng, C. Y.; Ayala, P. Y.; Chen, W.; Wong, M. W.; Andres, J. L.; Replogle, E. S.; Gomperts, R.; Martin, R. L.; Fox, D. J.; Binkley, J. S.; Defrees, D. J.; Baker, J.; Stewart, J. P.; Head-Gordon, M.; Gonzalez, C.; Pople, J. A. *Gaussian 94*; Revision C.2; Gaussian, Inc.: Pittsburgh, PA, 1995.
(35) Hehre, W. J.; Radom, L.; Schleyer, P. v. R.; Pople, J. A. *Ab Initio Molecular Orbital Theory*; Wiley-Interscience: New York, 1986.
(36) Becke, A. D. *J. Chem. Phys.* **1993**, *98*, 5648−5652.

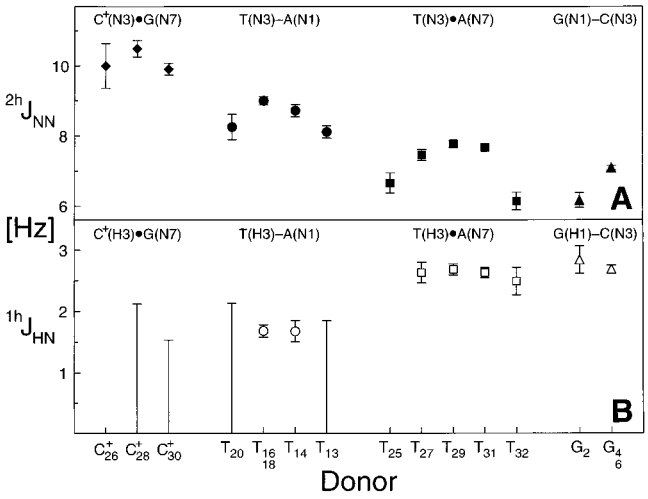

Figure 3. Calculated (A) $^{2h}J_{NN}$ and (B) $^{1h}J_{HN}$ coupling values from the quantitative J_{NN} HNN-COSY and the quantitative J_{HN} [^{1}H-^{15}N]-HSQC as a function of donor group. For the four base pair types, the two nuclei involved in the couplings are indicated at the top of panels A and B. Error bars correspond to propagated errors derived from the noise of the experiments. Values for J couplings of the overlapping T_{16}/T_{18} and G_4/G_6 resonances were determined as averages by using the intensities of the overlapped peaks. Upper limits for $^{1h}J_{HN}$ (shown as error bars without a central symbol) were derived for four unobserved correlations (C^+_{28}•G_4, C^+_{30}•G_6, $T_{20}-A_1$, and $T_{13}-A_8$) as described in the text. Quantification of an upper limit for the C^+_{26}•G_2 and the T_{25}•A_1 $^{1h}J_{HN}$ coupling was not possible due to low intensity and overlap in the reference spectrum, respectively.

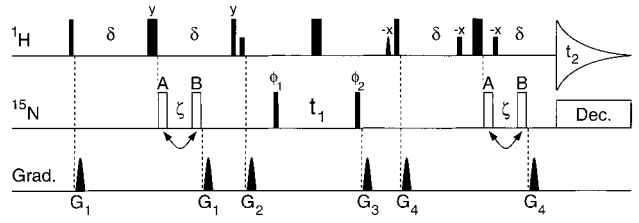

Figure 4. Pulse sequence of the quantitative J_{HN} [^{1}H-^{15}N]-HSQC experiment. Narrow and wide pulses correspond to flip angles of 90° and 180°, respectively. Carrier positions are ^1H_2O (^{1}H), 185 ppm (^{15}N), and 145 ppm (^{13}C). All regular ^{1}H and ^{15}N pulses are applied at a radio frequency field strength of 29 and 6.3 kHz, respectively. Rectangular low-power ^{1}H pulses are applied at a field strength of 200 Hz, and the sine-bell shaped $90°_{-x}$ pulse has a duration of 4.1 ms. Garp decoupling ($\gamma_C B_3/2\pi = 3.3$ kHz) was applied during the t_1 period on the ^{13}C channel and Waltz decoupling on the ^{15}N channel during acquisition ($\gamma_N B_2/2\pi = 1.25$ kHz). Delay durations: $\delta = 11.47$ ms; $\zeta = 2.87$ ms. Unless indicated, all pulses are applied along the x axis. Phase cycling: $\phi_1 = x, -x$; $\phi_2 = x, x, -x, -x$; receiver $= x, -x, -x, x$. Quadrature detection in the t_1 dimension was achieved by incrementing ϕ_1 in the States-TPPI manner. Gradients are sine-bell shaped, with an absolute amplitude of 25 G/cm at their center and durations (polarities) of $G_{1,2,3,4} = 0.2$ (+), 3.0 (+), 2.1 (−), and 0.4 (+). For the quantitation of J_{HN} couplings, two independent experiments are carried out with the ^{15}N 180° pulses applied at either position A or B. Cross-peaks observed for experiment A are mainly the result of small ^{1}H to ^{15}N couplings (such as $^{1h}J_{HN}$) which evolve during the full period 2δ. Cross-peaks observed in scheme B (reference) are the result of the strong $^1J_{NH}$ couplings which are active during the period $2(\delta - \zeta)$.

correlated Perdew−Wang 1991 correlation functional.[37,38] Magnetic shieldings were obtained via the GIAO method in the Gaussian 94 codes[39] at the B3PW91/6-311G** level of DFT. The ^{1}H chemical shifts are referenced to TMS via the value for CH_4 computed (31.61 ppm) at this level and the experimental TMS gas-phase value (0.13 ppm).[40]

Results and Discussion

$^{2h}J_{NN}$ Couplings. In addition to eight Watson−Crick base pairs, the DNA triplex depicted in Figure 1 contains five Hoogsteen[10,11] T•A and three Hoogsteen C^+•G base pairs, where + indicates protonation of C at N3. The HNN-COSY experiment[5] was used to detect hydrogen bonds involving the imino or iminium ion (H3−N3$^+$ of C^+) ^{15}N nuclei in these base pairs of the DNA triplex. For all four base pair types, and for all of the 16 hydrogen bonds involving an imino group as a donor and a nitrogen atom as an acceptor, trans-hydrogen bond $^{2h}J_{NN}$ correlations between the nitrogen donor and acceptor could be observed in the quantitative J HNN-COSY (Figure 2). The two top panels in this figure depict diagonal resonances (positive contours) corresponding to the imino (iminium) proton and nitrogen resonances of the hydrogen bond donor groups, i.e., T(^{1}H3−^{15}N3), G(^{1}H1−^{15}N1), and C^+(^{1}H3−^{15}N3). The bottom two panels show the cross correlations (negative contours) to the acceptor groups A(^{15}N1) and C(^{15}N3) for Watson−Crick T−A and G−C base pairs as well as A(^{15}N7) and G(^{15}N7) for the T•A and C^+•G Hoogsteen base pairs. Due to a very similar chemical environment, the base pairs G_4-C_{17}, G_6-C_{15} and $T_{16}-A_5$, $T_{18}-A_3$ have degenerate chemical shifts for both their diagonal and cross correlations. Additional resonances marked by an asterisk are the result of a minor second conformation of the DNA triplex (i.e., base pairs involving the first four purines A_1, G_2, A_3, and G_4). This second conformation constitutes approximately 15% of the total sample, as estimated from the intensity of the resonances. As previously noted for uridine, 5 weak intranucleotide correlations between the N3 and N1 nuclei of thymidine are also observed (negative contours, top panel).

Figure 3A shows the $^{2h}J_{NN}$ values determined from the intensity ratios of diagonal and cross-peaks in the HNN-COSY[5] as a function of donor base. Clearly, the four different types of base pairs lead to distinct differences in the strength of the trans-hydrogen bond $^{2h}J_{NN}$ couplings. The mean values for the $^{2h}J_{NN}$ couplings were 10.1 ± 0.3 Hz ($N = 3$) for Hoogsteen C^+•G, 8.5 ± 0.4 Hz ($N = 5$) for Watson−Crick T−A, 7.2 ± 0.7 Hz ($N = 5$) for Hoogsteen T•A, and 6.6 ± 0.6 Hz ($N = 3$) for Watson−Crick G−C base pairs. The coupling constants derived by this method contain minor systematic errors resulting from the finite strength of the ^{15}N radio frequency pulses and the large difference in chemical shifts of donor and acceptor groups. A numerical simulation shows that for the 10-kHz strength of the ^{15}N pulses used at a ^{15}N Larmor frequency of 50 MHz, the $^{2h}J_{NN}$ values are uniformly underestimated by 4.0−4.4% for Hoogsteen C^+•G, 5.1−5.6% for Watson−Crick T−A, and 3.8−7.1% for Hoogsteen T•A base pairs and overestimated by 1.5% for Watson−Crick G−C base pairs. These errors are similar in size to the statistical error determined from the spectral noise (Figure 3A, error bars) and no correction was made.

It is currently not possible to compare the measured $^{2h}J_{NN}$ values in Figure 3A with precise hydrogen bond donor−acceptor distances in DNA triplexes since such information is not yet available from either X-ray crystallography or NMR. A statistical analysis of three B-DNA dodecamer crystallographic structures at a resolution of <1.4 Å (NDB entries BD0007, BDJ019, and BDL084) and three DNA−protein complex structures at a resolution of 1.6 Å (PDB entries 1AAY, 1A1I, and 1AZP) shows that the variation of $R_{N1\cdots N3}$ distances in Watson−Crick base pairs is rather limited. In these structures,

(37) Wang, Y.; Perdew, J. P. *P. Phys. Rev. B* **1991**, *43*, 8911−8916.
(38) Wang, Y.; Perdew, J. P. *P. Phys. Rev. B* **1991**, *44*, 13298−13307.
(39) Barfield, M.; Fagerness, P. *J. Am. Chem. Soc.* **1997**, *119*, 8699−8711.
(40) Jameson, A. K.; Jameson, C. *J. Chem. Phys. Lett.* **1987**, *134*, 461−466.

the average $R_{N1\cdots N3}$ distance for G−C base pairs equals 2.92 ± 0.05 Å ($N = 44$) and is significantly larger than the $R_{N1\cdots N3}$ distance of 2.81 ± 0.05 Å ($N = 18$) for T−A base pairs. A recent crystallographic structure at 1.16 Å resolution of an acceptor stem of tRNAAla (NDB entry AR0009)[33] gives very similar results for Watson−Crick base pairs in RNA [GC: $R_{N1\cdots N3} = 2.91 \pm 0.08$ ($N = 8$); AU: $R_{N1\cdots N3} = 2.83 \pm 0.06$ ($N = 4$)]. This is in complete agreement with earlier studies at atomic resolution of base-paired adenylyl-3′-5′-uridine[41] and guanylyl-3′-5′-cytidine[42] with values of 2.82 and 2.95 Å for U−A and G−C $R_{N1\cdots N3}$ distances, respectively. Very limited high-precision information on hydrogen bond distances is available for Hoogsteen base pairs. To the best of our knowledge, precise data on C^+•G base pairs are currently not available. An early neutron diffraction study of 9-methyladenine•1-methylthymine[43] gave values of 2.93 Å for $R_{T(N3)\cdots A(N7)}$ and 1.044 Å for $R_{T(N3)-T(H3)}$ in a T•A Hoogsteen base pair. Under the assumption that the hydrogen bond distances between nitrogen donor and acceptor atoms in the DNA triplex are close to the observed crystallographic distances of 2.81 ± 0.05 (T−A), 2.93 (T•A), 2.92 ± 0.05 Å (G−C), it is striking that the shorter donor−acceptor distances in the T−A base pairs are correlated with a stronger $^{2h}J_{NN}$ coupling constant. Similar observations have been made for the $^{2h}J_{NN}$ in Watson−Crick RNA base pairs.[5] Although part of these variations may be due to the different chemical nature of the donor and acceptor groups in the different base types, the results of DFT calculations of this coupling (vide infra) as a function of hydrogen bond length are consistent with the concept that an increased overlap between the 1s atomic orbital of the imino proton and a trigonal hybrid orbital of the nitrogen acceptor atom leads to an increase in the value of $^{2h}J_{NN}$.

As is evident from Figure 3A, there is a distinct decrease of about 1−1.6 Hz in the values of the $^{2h}J_{NN}$ couplings for the four Watson−Crick and Hoogsteen T/A base pairs located at each end of the DNA triplex ($T_{20}-A_1$, $T_{13}-A_8$, $T_{25}•A_1$, and $T_{32}•A_8$). Since the observed couplings represent a time and ensemble average over the states of the molecule, this means that the average electronic interaction in the hydrogen bonds is reduced at these positions. Such a reduction could be due to an increased static distance between donor and acceptor or to a shift of the dynamic equilibrium between closed and open states of the base pairs toward the open state. Note that an increased exchange of the imino proton with the solvent will not affect the determined value for the $^{2h}J_{NN}$ couplings in the quantitative HNN-COSY experiment because both cross and diagonal peak intensities would be reduced by the same relative amount. The notion that the $^{2h}J_{NN}$ couplings provide a meaningful characterization of subtle variations in the hydrogen bond is supported by the fact that the largest reduction in the $^{2h}J_{NN}$ coupling (1.6 Hz) occurs between the last two base pairs ($T_{31}•A_7$ and $T_{32}•A_8$) at the 3′-end of the triplex. Apparently, the loosening of the hydrogen bond is less hindered at this end of the exterior third strand than at the 5′-end of the triplex ($T_{25}•A_1$), which is embedded within the closed loop connecting the second and third strand.

Compared to the cross-peaks arising from the other base pair groups, the acceptor ^{15}N nuclei of Hoogsteen T•A base pairs in Figure 2 have a much larger chemical shift dispersion. In particular, the 5′- and 3′-terminal Hoogsteen T•A acceptor peaks, A1(^{15}N7) and A8(^{15}N7), are downfield shifted by about 5−7 ppm with respect to the resonances arising from the more interior A3(^{15}N7) and A5(^{15}N7) acceptors at approximately 225 ppm. It has been noted previously that the formation of a Hoogsteen T•A base pair causes the chemical shift of the acceptor adenosine $^{15}N7$ nucleus to move upfield from approximately 233 to 226 ppm.[44] Therefore the downfield shift of A1(^{15}N7) and A8(^{15}N7) is an additional indication for the loosening of hydrogen bonds at both termini of the triplex. In contrast, the ^{15}N chemical shift dispersion is not as large for the G(^{15}N7) hydrogen bond acceptor in the chemically very similar Hoogsteen C^+•G base pairs of the triplex. Most likely, there is less variation for the C^+•G base pairs, as these residues are located in the central portion of the DNA structure where they are much less affected by fraying.

The intensities of the four intraresidue $^2J_{N3N1}$ correlations observed for thymidine (Figure 2, top panel) yield a mean value for this two-bond coupling of 2.6 ± 0.4 Hz, which is in agreement with previously reported values for monomeric[45] and base paired[5] uridine nucleotides. A very weak cross-peak is observed from the iminium ion group of C^+_{30} to a ^{15}N resonance at approximately 153 ppm (data not shown). On the basis of its chemical shift,[46] this correlation was assigned to an intraresidue two-bond transfer from the N3 to the N1 nucleus of the protonated cytidine. The value for this $^2J_{N3N1}$ coupling is 3.8 ± 1.5 Hz (error estimated from the spectral noise level). Intraresidue transfers from the N1 to the N3 nucleus of guanosine ($^2J_{N1N3}$) were below the detection limit. However, an upper limit of 1.8 Hz was calculated for this coupling from the ratio of the height of the lowest plotted contour line relative to the amplitude of the diagonal peak.

$^{1h}J_{HN}$ Couplings. Recently, trans-hydrogen bond couplings, $^{1h}J_{HN}$, between the proton and the acceptor nitrogen have been observed in a ^{15}N-labeled DNA duplex by using an E.COSY based approach.[6] Values for these coupling constants are in the range of 1.8−3.6 Hz. Here we report a simple experimental scheme to observe and quantify these couplings by a modification of a standard water flip-back [^{1}H-^{15}N]-HSQC experiment (Figure 4).[28] In the standard HSQC, the time, 2δ, for the INEPT and reverse INEPT transfers between the in-phase H_y and the anti-phase $2H_xN_z$ magnetization is usually set to values slightly shorter than $1/(2*^1J_{NH})$ or approximately 5 ms. In the modified [^{1}H-^{15}N]-HSQC experiment (Figure 4, scheme A), the value of 2δ was set to 22.9 ms, i.e., close to $2/^1J_{NH}$. This has the effect of approximately refocusing the covalent $^1J_{NH}$ coupling during the INEPT transfers, but leaving the transfer from the imino proton to the acceptor nitrogen by the much smaller $^{1h}J_{HN}$ couplings active. In principle, any choice of $2\delta \approx n/^1J_{NH}$, with n being an integer, would achieve this effect. However, maximal sensitivity for the cross-peaks is achieved when 2δ is set to values close to the transverse relaxation time of the imino proton. In addition to the two one-bond couplings $^1J_{NH}$ and $^{1h}J_{HN}$, intraresidue three-bond couplings ($^3J_{NH}$) are active during the INEPT transfers in the [^{1}H-^{15}N]-HSQC. These are $^3J_{H3N1}$ for thymidine and protonated cytidine bases (see insert to Figure 5B) and $^3J_{H1N3}$ for guanosine. Note that the three-bond couplings from the protons to the amino ^{15}N nuclei are effectively decoupled because of the limited radio frequency strength of the nitrogen 180° pulses. As a result of all the active couplings,

(41) Seeman, N. C.; Rosenberg, J. M.; Suddath, F. L.; Kim, J. J. P.; Rich, A. *J. Mol. Biol.* **1976**, *104*, 109−144.
(42) Rosenberg, J. M.; Seeman, N. C.; Day, R. O.; Rich, A. *J. Mol. Biol.* **1976**, *104*, 145−167.
(43) Frey, M. N.; Koetzle, T. F.; Lehmann, M. S.; Hamilton, W. C. *J. Chem. Phys.* **1973**, *59*, 915−924.
(44) Gaffney, B. L.; Kung, P.-P.; Wang, C.; Jones, R. A. *J. Am. Chem. Soc.* **1995**, *117*, 12281−12283.
(45) Büchner, P.; Maurer, W.; Rüterjans, H. *J. Magn. Reson.* **1978**, *29*, 45−63.
(46) Markowski, V.; Sullivan, G. R.; Roberts, J. D. *J. Am. Chem. Soc.* **1977**, *99*, 714−718.

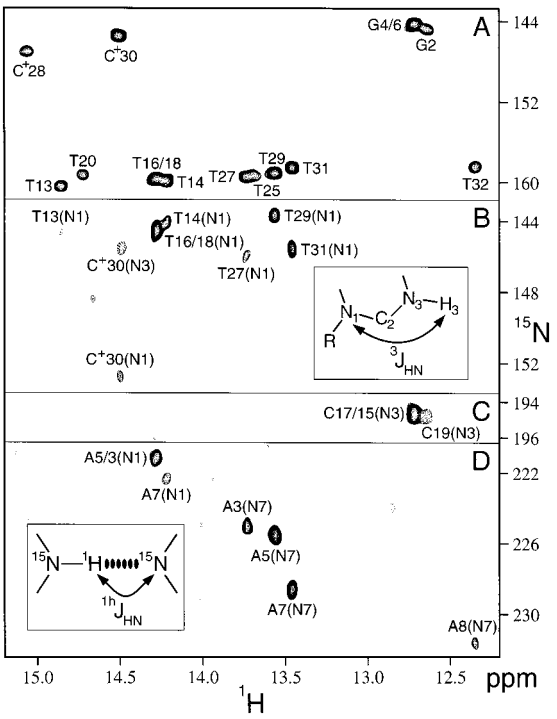

Figure 5. Quantitative J_{HN} [^{15}N-^{1}H]-HSQC spectra of the uniformly ^{15}N/^{13}C-labeled intramolecular DNA triplex. Resonances are labeled with assignment information. (A) Reference spectrum recorded by using pulse scheme B of Figure 4 showing covalent one-bond imino and iminium ion group correlations. (B, C, D) Resonances observed from recording a spectrum with pulse scheme A in Figure 4. Panel B shows three-bond intranucleotide scalar coupling correlations ($^{3}J_{HN}$; see insert in panel B for definition) between H3 and N1 of thymidine and protonated cytidine bases. The negative resonance (dashed lines) marked C^{+}_{30} (N3) is a result of the incomplete refocusing of the intraresidue $^{1}J_{N3H3}$ coupling. Resonances in panel C result from magnetization transfer across the hydrogen bond between the proton and acceptor nitrogen nuclei for Watson−Crick G−C base pairs. Panel D shows resonances arising from magnetization transfer between the proton and acceptor nitrogen in Watson−Crick T−A ($A_{5/3}$ and A_7) and Hoogsteen T•A (A_3, A_5, A_7, and A_8) base pairs. The insert illustrates the definition of the scalar $^{1h}J_{HN}$ correlation via the hydrogen bond. The heights of contour lines in panels B−D are drawn at the same scale, whereas the contour lines in panel A are drawn at 8.8 times higher level (corrected for different total experimental time).

the intensity of a cross-peak between the imino proton and the nitrogen acceptor nucleus in the modified HSQC (Figure 4, scheme A) will be proportional to $\sin^2(2\pi^{1h}J_{HN}\delta)\cos^2(2\pi^{1}J_{NH}\delta)\cos^2(2\pi^{3}J_{HN}\delta)$.

To determine the size of the $^{1h}J_{HN}$ coupling in a quantitative manner, a second [^{1}H-^{15}N]-HSQC experiment was recorded with the same total length 2δ for the INEPT and reverse INEPT periods, but with the ^{15}N 180° pulses shifted by a delay ζ = 2.87 ms $\approx 1/(4*^{1}J_{NH})$ relative to the position of the ^{1}H 180° pulses in the middle of the INEPT transfer intervals (reference experiment, scheme B in Figure 4). This has the effect of reducing the effective duration for the ^{1}H to ^{15}N defocusing and refocusing periods to $2*(\delta-\zeta) \approx 3/(2*^{1}J_{NH})$ while keeping the relaxation losses identical to the experiment of pulse scheme A. In this reference experiment, the intensities of the $^{1}J_{NH}$ cross-peaks will be proportional to $\sin^2(2\pi^{1}J_{NH}[\delta-\zeta])\cos^2(2\pi^{1h}J_{HN}[\delta-\zeta])\cos^2(2\pi^{3}J_{HN}[\delta-\zeta])$. Therefore, the ratio of the intensities of the $^{1h}J_{HN}$ correlation in scheme A relative to the $^{1}J_{NH}$ correlation of scheme B is given by

$$\frac{I_{hbond}}{I_{ref}} = \left(\frac{\sin(2\pi^{1h}J_{HN}\delta)\cos(2\pi^{1}J_{HN}\delta)\cos(2\pi^{3}J_{HN}\delta)}{\sin(2\pi^{1}J_{HN}[\delta-\zeta])\cos(2\pi^{1h}J_{HN}[\delta-\zeta])\cos(2\pi^{3}J_{HN}[\delta-\zeta])}\right)^2 \quad (1)$$

For small values of $^{1h}J_{HN}$ and $^{3}J_{HN}$ as well as values of $^{1}J_{NH}$ close to $1/\delta$, such that $|2\pi^{1h}J_{HN}\delta|$, $|2\pi^{3}J_{HN}\delta| \ll 1$ and $|(^{1}J_{NH}[\delta-1])2\pi| \ll 1$, this expression can be approximated by $I_{hbond}/I_{ref} \approx (2\pi^{1h}J_{HN}\delta)^2$. In the present case, for variations of $^{1}J_{NH}$ of less than 4 Hz from $1/\delta$ and values of $|^{1h}J_{HN}|$ and $|^{3}J_{HN}|$ smaller than 4 Hz, this approximation leads to errors of less than 5% in the determination of the $^{1h}J_{HN}$ coupling constant. In an analogous way, values for the intraresidue $^{3}J_{HN}$ couplings can be derived from the ratio of the intraresidue $^{3}J_{HN}$ cross-peak intensities relative to the intensity of the $^{1}J_{NH}$ correlation in the reference experiment.

Figure 5B−D shows the results of the quantitative J_{HN} [^{1}H-^{15}N]-HSQC experiment (pulse scheme A) for the DNA triplex. A total of 10 out of 16 possible trans-hydrogen bond $^{1h}J_{HN}$ correlations could be observed (Figure 5, panels C and D). As in the case of the $^{2h}J_{NN}$ correlations, bases G_4/G_6 and T_{16}/T_{18} are indistinguishable in both their cross and diagonal resonances. In addition, a number of intraresidue $^{3}J_{H3N1}$ correlations are observed (Figure 5B). The variation in the $^{1}J_{NH}$ coupling constants is the cause for an incomplete suppression of the intraresidue one-bond H3−N3 correlations for some of the T and C^{+} residues (data not shown, except for C^{+}_{30}(N3)). For comparison, the result of the reference $^{1}J_{NH}$ HSQC (pulse scheme B) is depicted in Figure 5A.

Values for the trans-hydrogen bond $^{1h}J_{HN}$ couplings determined by the quantitative J_{HN} [^{1}H-^{15}N]-HSQC are shown in Figure 3B as a function of donor base. The couplings range from approximately 1.7 to 2.8 Hz for Watson−Crick T−A, Watson−Crick G−C, and Hoogsteen T•A base pairs. This is in agreement with recently published results for DNA Watson−Crick base pairs.[6] The two terminal Watson−Crick T−A base pairs ($T_{20}-A_1$, $T_{13}-A_8$) and one terminal Hoogsteen T•A base pair (T_{25}•A_1) $^{1h}J_{HN}$ correlations were below the detection limit, probably as a result of fraying of the strands' termini as explained in the discussion of the $^{2h}J_{NN}$ correlations. Upper limits for such unobserved $^{1h}J_{HN}$ correlations (besides T_{25}•A_1 and C^{+}_{26}•G_2) were estimated from the ratio of the height of the lowest plotted contour line in the spectrum recorded with pulse scheme A relative to the amplitude of the diagonal peak in the reference spectrum (Figure 5A). As in the case of the $^{2h}J_{NN}$ correlation, some error is introduced in the determination of $^{1h}J_{HN}$ by the quantitative J_{HN} [^{1}H-^{15}N]-HSQC due to the finite strength of the ^{15}N radio frequency pulses and the large offsets of the ^{15}N donor and acceptor nuclei. A numerical simulation shows that this introduces an underestimation by approximately 10% in $^{1h}J_{HN}$ for the T−A and T•A base pairs and an overestimation by 16% in $^{1h}J_{HN}$ for the G−C base pairs. These errors were not corrected for in Figure 3B.

Seven intraresidue $^{3}J_{H3N1}$ correlations were observed for the thymidine or protonated cytidine bases (Figure 5B). The mean value for this $^{3}J_{H3N1}$ coupling is 2.0 ± 0.1 Hz. Intraresidue three-bond transfers from the H1 to the N3 nucleus of guanosine, $^{3}J_{H1N3}$, are below the detection limit. The upper limit calculated for this $^{3}J_{H1N3}$ coupling is 2.1 Hz.

Correlations between $^{1h}J_{HN}$, $^{2h}J_{NN}$, and $^{1}J_{NH}$ and the Proton Chemical Shift. Figure 6A shows that irrespective of the base pair type there is a strong linear correlation (r = 0.86)

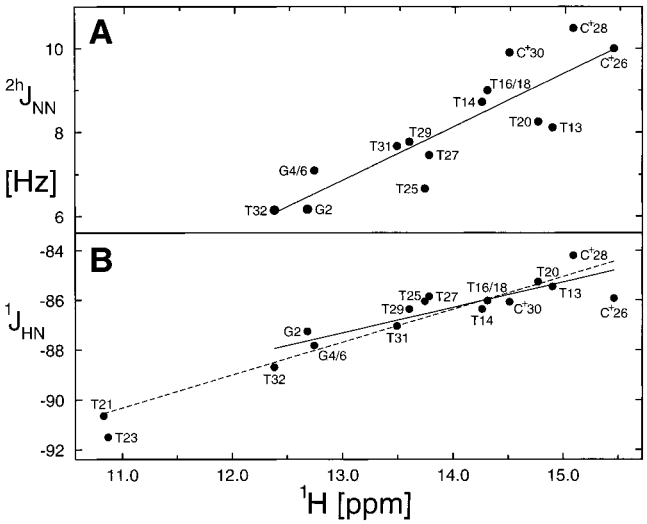

Figure 6. Correlations between $^{2h}J_{NN}$ (A) and $^{1}J_{HN}$ (B) couplings and the isotropic shift of the imino proton δ_H. The labeling of symbols corresponds to the residue numbering of the intramolecular DNA triplex. The continuous lines in panels A and B correspond to linear regressions including all the data points from base pairs with nitrogen atoms as hydrogen bond acceptors (see text). The dashed line corresponds to a linear regression of $^{1}J_{HN} = (-1.32\ \text{Hz/ppm})\delta_H + 104.79$ Hz ($r = 0.94$), which was calculated over all hydrogen-bonded imino groups including T_{21}(H3−N3) and T_{23}(H3−N3). Errors in the determination of $^{2h}J_{NN}$ are identical to Figure 3A, whereas errors for the determination of $^{1}J_{HN}$ were determined previously as <0.2 Hz for similar sized molecules.[30] Reproducibility in the chemical shift measurements is better than 0.03 ppm.

between the isotropic chemical shift δ_H of the imino proton and the $^{2h}J_{NN}$ coupling. A downfield shift of the imino proton corresponds to a larger value in $^{2h}J_{NN}$. In proteins, downfield shifts of the amide proton correlate with shorter hydrogen bond donor−acceptor distances.[14−20] In addition, such a deshielding of the amide proton correlates with larger values of the recently observed protein trans-hydrogen bond couplings ($^{3h}J_{NiC'j}$).[9a] These parallel results in nucleic acids and proteins provide additional evidence that the strengths of the trans-hydrogen bond couplings $^{2h}J_{NN}$ and $^{3h}J_{NiC'j}$ are a direct measure for the hydrogen bond length, where stronger couplings are indicative of shorter donor−acceptor distances.

Figure 6B shows that there is also a strong linear correlation (solid line, $r = 0.94$) between the imino proton chemical shift and the $^{1}J_{NH}$ coupling constant for imino groups bonded to a nitrogen acceptor. The $^{1}J_{NH}$ couplings range from approximately −84 to −89 Hz where a decrease in the absolute size of the couplings correlates with a downfield shift for the imino proton. Thus, the $^{1}J_{NH}$ couplings are also correlated to the size of $^{2h}J_{NN}$ and presumably to the strength of the hydrogen bond. Similar variations in $^{1}J_{NH}$ couplings of approximately 4 Hz upon hydrogen bond formation have been observed in a number of chemical systems.[47−49] In particular, for an adenosine−uridine base pair analogue in chloroform, the formation of the base pair resulted in a decrease of $|^{1}J_{NH}|$ from 91.3 to 87.5 Hz.[50] Preliminary results which are derived from perturbation theory and an independent electron model[51] for a three-orbital N1−H1···N3 fragment indicate that $|^{1}J_{NH}|$ and $^{2h}J_{NN}$ respectively should decrease and increase approximately quadratically with the overlap integral between H1 and N3.

Chart 1

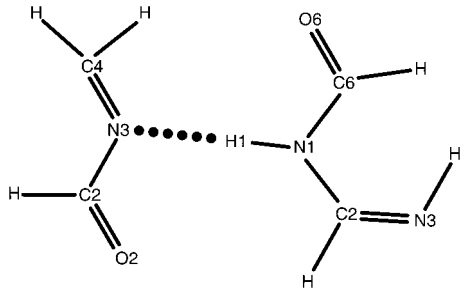

The strongest $^{1}J_{NH}$ couplings (−90.6 and −91.5 Hz) in Figure 6B are observed for the two thymidines positioned in the second loop of the DNA triplex (T_{21}, T_{23}; see Figure 1). The imino groups of these two bases show no significant exchange with the solvent at 5 °C and no trans-hydrogen bond $^{2h}J_{NN}$ correlations. Thus the imino protons of T_{21} and T_{23} are most likely hydrogen bonded to nearby DNA oxygen atoms instead of nitrogen atoms. At this point, we have not performed any DFT calculations (see below) that would describe the behavior of hydrogen-bonded systems with oxygen as the acceptor atom. It is, however, remarkable that the data points for T_{21} and T_{23} in Figure 6B seem to follow a similar linear trend (shown as dashed line) as the nitrogen-bonded imino groups. A similar increase in the strength of the imino $^{1}J_{NH}$ couplings is observed in RNA G−U base pairs where the hydrogen bond acceptor is also an oxygen atom (A. J. Dingley, unpublished results).

Density Functional Calculations of Scalar Coupling and Magnetic Shielding Associated with Hydrogen Bonding in a G−C Base Pair Fragment. It was of interest to examine the dependency of the trans-hydrogen bond couplings and the chemical shifts on structural parameters in hydrogen-bonded base pairs by theoretical methods. In general, the Fermi contact contributions dominate the nuclear spin−spin couplings, but these are exceedingly sensitive to the inclusion of electron correlation effects.[52,53] For this reason, density functional theory[21,22] seems ideally suited to the problem. The use of DFT methods greatly extends the size of molecules which can be examined with the inclusion of electron correlation effects.[53,54] A recent study,[54] using DFT methods and finite perturbation theory,[23,24] gave excellent agreement with the experimental spin−spin couplings in a very large number of different polyhedral carboranes. Computations of magnetic shielding primarily make use of distributed origins algorithms such as GIAO methods.[25] For example, a recent DFT/GIAO study gave results in good agreement with experimental ^{13}C, ^{15}N, and ^{1}H chemical shifts in pharmacologically important aminopyrimidines,[39] and these were found to be related to electron densities and amine group orientations.

The size of an entire base pair makes it untractable for a systematic variation of geometrical parameters in DFT calculations. Depicted in Chart 1 is a 16-atom fragment of a Watson−Crick G−C base pair. This fragment retains the electronic and

(47) Paolillo, L.; Becker, E. D. *J. Magn. Reson.* **1970**, *2*, 168−173.
(48) Axenrod, T.; Pregosin, P. S.; Wieder, M. J.; Becker, E. D.; Bradley, R. B.; Milne, G. W. A. *J. Am. Chem. Soc.* **1971**, *93*, 6536−6541.
(49) Axenrod, T.; Wieder, M. J. *J. Am. Chem. Soc.* **1971**, *93*, 3541−3542.
(50) Poulter, C. D.; Livingston, C. L. *Tetrahedron Lett.* **1979**, *9*, 755−758.
(51) Barfield, M. In preparation.
(52) Barfield, M. *Encyclopedia of Nuclear Magnetic Resonance*; Grant, D. M., Harris, R. K., Eds.; John Wiley: New York, 1996; pp 2520−2532.
(53) Theoretical aspects of nuclear spin−spin coupling have been reviewed annually starting in 1972: Fukui, H. In *Nuclear Magnetic Resonance*; Specialist Periodical Reports; The Chemical Society: London. 1997; No. 26 and previous chapters in this series.
(54) Onak, T.; Jaballas, J.; Barfield, M. *J. Am. Chem. Soc.* **1999**, *121*, 2850−2856.

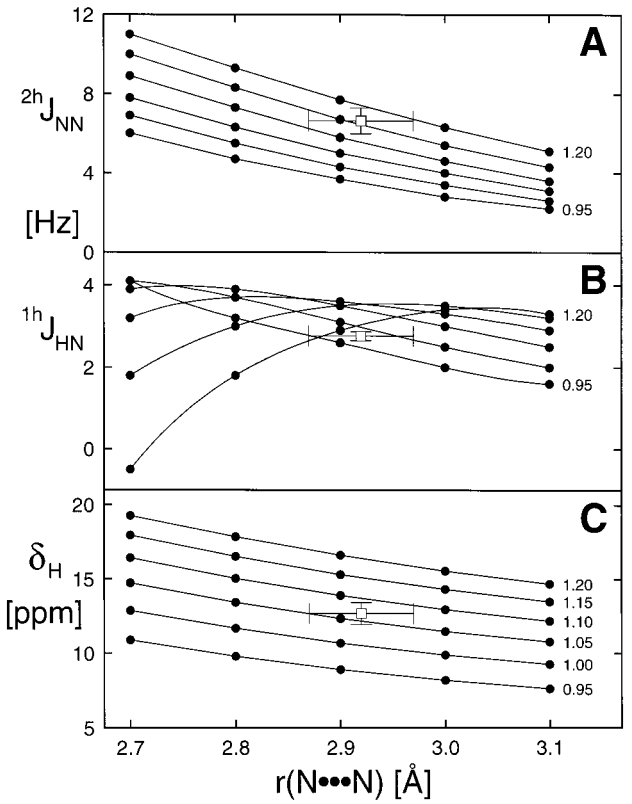

Figure 7. $^{2h}J_{N1N3}$ (A) and $^{1h}J_{H1N3}$ (B) coupling constants and the imino proton chemical shift δ_{H1} (C) calculated from DFT for the G−C base pair fragment (Chart 1) as a function of the $R_{N1\cdots N3}$ and R_{N1-H1} distances. The data represent R_{N1-H1} values of 0.95, 1.00, 1.05, 1.10, 1.15, and 1.20 Å (marked at the right). Data points depicted by open boxes and error bars correspond to mean values and deviations for $R_{N1\cdots N3}$ distances observed in DNA crystal structures and to the experimentally observed mean values and deviations for $^{2h}J_{N1N3}$ (A), $^{1h}J_{H1N3}$ (B), and δ_{H1} (C) for the G−C base pairs in the DNA triplex.

nuclear structure in the hydrogen-bonding region and was chosen as a model for DFT calculations of coupling constants and chemical shifts as a function of the hydrogen bond parameters $R_{N1\cdots N3}$ and R_{N1-H1}. To reduce the number of structural variables, it was further assumed that N1−H1···N3 is linear.

The Fermi contact contributions to the $^{2h}J_{N1N3}$, $^{1h}J_{H1N3}$, and $^{1}J_{N1H1}$ coupling constants and the isotropic magnetic shieldings were computed at 0.05-Å intervals for R_{N1-H1} (0.95−1.20 Å) and at 0.1-Å intervals for $R_{N1\cdots N3}$ (2.7−3.1 Å). For these values of $R_{N1\cdots N3}$, the calculated equilibrium distances R_{N1-H1} range from 1.033 to 1.023 Å for the 16-atom G−C model. In comparison, equilibrium values of 1.038 and 1.050 Å for the covalent imino group bond length were computed for full G−C and U−A base pairs, respectively.[51]

The calculated $^{2h}J_{N1N3}$, $^{1h}J_{H1N3}$ coupling constants and the imino proton chemical shift δ_{H1} are plotted in Figure 7, panels A, B, and C, as functions of the $R_{N1\cdots N3}$ distance for values of R_{N1-H1} in the range 0.95−1.20 Å. It is clearly visible that a decrease in $R_{N1\cdots N3}$ results in increased values of both $^{2h}J_{N1N3}$ (Figure 7A) and δ_{H1} (Figure 7C) for all values of R_{N1-H1} considered. The effect on $^{1h}J_{H1N3}$ (Figure 7B) is variable: for $R_{N1-H1} > 1.10$ Å, $^{1h}J_{N3H1}$ increases with increasing $R_{N1\cdots N3}$ whereas for smaller values of R_{N1-H1} a decrease is observed.

A direct comparison of the calculated parameters to the experimental data is hampered by the absence of precise information on the hydrogen bond distances in the DNA triplex. However, assuming a value of 2.92 Å for $R_{N1\cdots N3}$ and of 1.038 Å for R_{N1-H1} in the G−C base pair, the experimentally observed couplings $^{2h}J_{N1N3}$, $^{1h}J_{H1N3}$ and the imino proton chemical shift are closely reproduced by the DFT calculation (Figure 7). Part of the remaining discrepancies between experimental and calculated data can be attributed to the incompletely considered chemical structure of the G−C base pair, to the neglect of the non Fermi contact contributions to the scalar couplings, and to ring current effects on the chemical shift. A serious additional source of error arises from the fact that the coupling constants are computed for fixed internuclear distances, while the experimental data reflect averaging over the vibrational motions. This effect is particularly strong in the determination of the covalent coupling constant $^{1}J_{N1H1}$. Similar to recent results for other types of $^{1}J_{XH}$ couplings,[54,55] the calculated values are underestimated in absolute size by 10−20% for the equilibrium hydrogen bond distances (data not shown). However, a clear trend is also observed for these $^{1}J_{N1H1}$ coupling constants which are in the range of −60.0 to −90.1 Hz for the bond lengths considered: shorter $R_{N1\cdots N3}$ distances lead to smaller (absolute size) $^{1}J_{N1H1}$ couplings whereas shorter R_{N1-H1} distances have the opposite effect.

The DFT calculations yield positive values for both $^{2h}J_{N1N3}$ and $^{1h}J_{H1N3}$ couplings and negative values for the $^{1}J_{N1H1}$ couplings. This is in complete agreement with experimental observations for the sign of normal $^{1}J_{NH}$ couplings[56] and of $^{1h}J_{HN}$.[6] Due to the limitations of the quantitative *J* HNN-COSY experiment, the sign of $^{2h}J_{NN}$ had not been determined before.[5] Results of an E.COSY experiment indicate, however, that the sign of $^{2h}J_{NN}$ is also positive (A. Dingley, unpublished results) and in agreement with the calculations.

DFT calculations of the imino proton equilibrium position indicate that the R_{N1-H1} distance is not strongly influenced ($<\sim$0.01 Å) by the variation of $R_{N1\cdots N3}$ within the 2.7−3.1 Å range or by the base pair type considered (see above). The experimentally observed linear correlation between $^{2h}J_{N1N3}$, $^{1}J_{N1H1}$ and the imino proton chemical shift δ_{H1} extends over all four base pair types of the DNA triplex (Figure 6). This seems to indicate that the mechanism responsible for the observed variations in these parameters is identical in all base pair types. In addition, preliminary DFT/GIAO calculations on different base pair types[51] show that there is only a minor contribution from the different chemical nature of donor and acceptor groups to the values of $^{2h}J_{N1N3}$, $^{1}J_{N1H1}$, and δ_{H1}. For these reasons, it is very likely that most of the experimentally observed variations in these parameters are caused by changes in the donor−acceptor distance $R_{N1\cdots N3}$.

Under the assumption of a sole dependence of $^{2h}J_{N1N3}$, $^{1}J_{N1H1}$, and δ_{H1} on $R_{N1\cdots N3}$, the DFT calculations reproduce the experimental trends surprisingly well. For example, the correlations between calculated values for $^{2h}J_{N1N3}$, $^{1}J_{N1H1}$, and the chemical shift δ_{H1} are very nearly linear in conformity with the experimental results in Figure 6A,B. A regression analysis of the calculated data [at R_{N1-H1}= 1.05 Å] provides the following:

$$^{2h}J_{N1N3}(\text{calc}) = (1.17\ \text{Hz/ppm})\delta_{H1} - 9.4\ \text{Hz}\ (r = 0.9999)$$

$$^{1}J_{H1N1}\ (\text{calc}) = (1.01\ \text{Hz/ppm})\delta_{H1} - 91.9\ \text{Hz}\ (r = 0.9844)$$

(55) Bennett, B.; Raynes, W. T.; Anderson, C. W. *Spectrochim. Acta, Ser. A* **1989**, *48*, 821−827.
(56) Chuck, R. J.; Gillies, D. G.; Randall, E. W. *Mol. Phys.* **1969**, *16*, 121−130.

This is in close agreement with a regression analysis of the data observed for the base pairs with nitrogen atoms as hydrogen bond acceptors in Figure 6B (solid line):

$$^{2h}J_{NN}(\text{exp}) = (1.27\ \text{Hz/ppm})\delta_{H1} - 9.6\ \text{Hz}\ (r = 0.861)$$

$$^{1}J_{HN}(\text{exp}) = (1.02\ \text{Hz/ppm})\delta_{H1} - 100.6\ \text{Hz}\ (r = 0.864)$$

Concluding Remarks

The results described herein are the first extensive set of measurements of coupling constants related to the hydrogen bonds in four different types of DNA base pairs. Trans-hydrogen bond scalar couplings could be observed not only for Watson−Crick base pairs but also between the donor and acceptor groups of Hoogsteen T•A and C^+•G base pairs. Variations in the values of both $^{2h}J_{NN}$ and $^{1}J_{NH}$ are strongly correlated to the imino proton chemical shift. Due to fraying of the DNA triplex stem ends, a distinct decrease in $^{2h}J_{NN}$ values is observed for nucleic acid base pairs located at these positions. The results should be useful for the characterization of the strength of the hydrogen bond in other macromolecular nucleic acid systems.

Density functional methods were used to calculate scalar couplings and chemical shifts for a 16-atom model of a Watson−Crick G−C base pair as a function of hydrogen bond distances. This permits a systematic investigation of the distance dependence of the NMR parameter in the trans-hydrogen bond region. Considering the complexity and size of this base pair fragment, the correspondence between the calculated and experimental results is very reasonable. It is concluded that this fragment and the method of computation adequately represent the key factors of the electronic interactions in a hydrogen bond of the N−H···N type. These interactions explain in a quantitative way the trans-hydrogen bond scalar coupling effect and the experimental trends observed for the coupling constants and chemical shifts of the nuclei involved in the hydrogen bond.

Acknowledgment. We thank Udo Heinemann and Uwe Müller for the making the tRNAAla crystal structure available to us prior to publication. A.J.D. is a recipient of an Australian National Health and Medical Research Council C.J. Martin Fellowship (Regkey 987074). This work was funded by DFG grant GR1683/1-1 to S.G. and NIH grants GM37254 and GM48123 to J.F.

JA9908321